Cell Reports
Physical Science

CellPress
OPEN ACCESS

Article

Conceptualizing novel CH_3OH-based thermochemical energy storage routes via a modeling approach

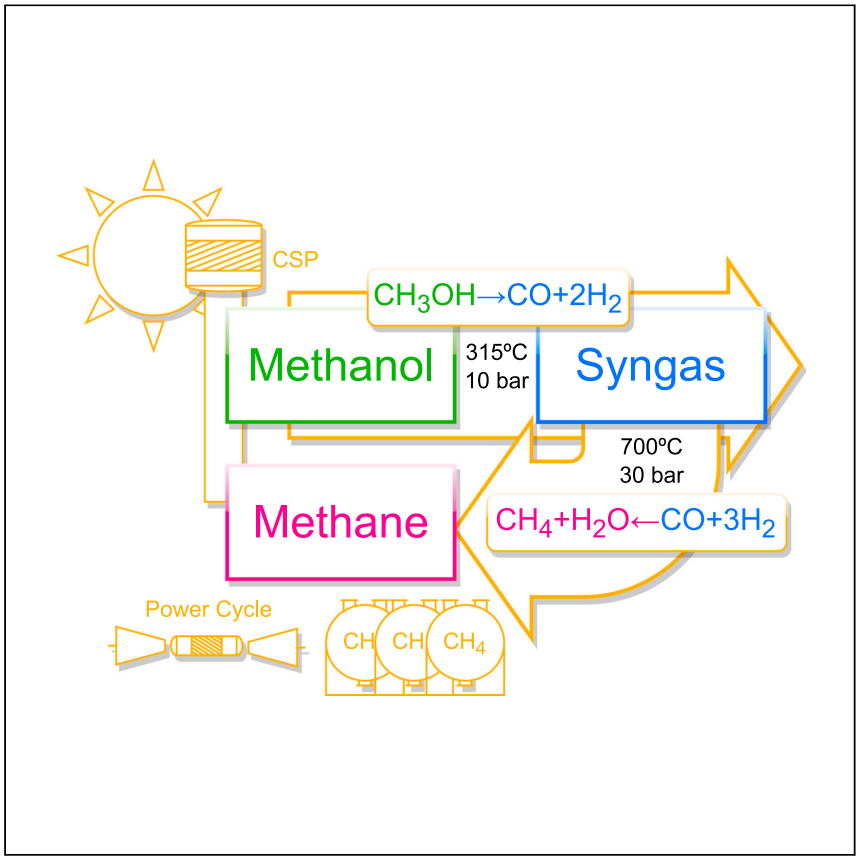

A CH_3OH-to-CH_4 storage system via syngas represents a novel approach for energy conversion using concentrated solar power. Here, Rodriguez-Pastor et al. propose a storage system where the resulting CH_4 is of high molar fraction and can be utilized in existing technologies, offering greater energy storage density due to the liquid state of CH_3OH.

Diego Antonio Rodriguez-Pastor, Andrés Carro, Giuseppe Masci, Carlos Ortiz, Vittorio Verda, Ricardo Chacartegui

drodriguez4@us.es (D.A.R.-P.)
ricardoch@us.es (R.C.)

Highlights

A CH_3OH-to-CH_4 storage system is proposed

Thermal efficiencies greater than 40% are obtained through solar integration

CH_4 is produced in greater than 70% molar fraction, usable in existing technologies

Competitive levelized storage costs with other thermal energy storage systems are shown

Rodriguez-Pastor et al., Cell Reports Physical Science 4, 101357
April 19, 2023
https://doi.org/10.1016/j.xcrp.2023.101357

Cell Reports
Physical Science

CellPress
OPEN ACCESS

Article

Conceptualizing novel CH_3OH-based thermochemical energy storage routes via a modeling approach

Diego Antonio Rodriguez-Pastor,[1,*] Andrés Carro,[1] Giuseppe Masci,[1,3] Carlos Ortiz,[2] Vittorio Verda,[3] and Ricardo Chacartegui[1,4,5,*]

SUMMARY

Thermal energy storage systems are an emerging option for efficient energy conversion and storage, especially if they can concentrate solar energy. This work studies a flexible CH_3OH-to-CH_4 conversion system from intermediate conversion to synthesis gas. The design is based on a combination of processes already tested experimentally and applied in industry. The concept we develop integrates the decomposition of CH_3OH and methanation processes, providing different pathways for energy use, such as natural gas, direct heat, and power supply, or storage in chemical bonds. This flexibility in adapting the operation of the system to different energy availability and energy needs makes the concept appealing for changeable application. Thermal efficiencies of 39% are possible for the CH_3OH decomposition phase and of 26% for the overall system for CH_4 production. Thus, from the high energy density of CH_3OH, levelized storage costs of €134.8/MWh can be obtained, which is lower than systems based on molten salts. These results should spur interest in further advances for the proposed flexible concept.

INTRODUCTION

Increasing the energy storage capacity of renewable energy systems is currently a key challenge.[1] Costs of photovoltaics (PVs), wind, and even concentrating solar power (CSP) are currently competitive with fossil fuels,[2] although dispatchability is a major issue. According to IRENA,[3] the global energy storage capacity should increase from 30 GWh today to more than 9,000 GWh by 2050 to meet the COP21 agreement.[4] To achieve this ambitious goal, several technologies and energy storage paths must be developed on a large scale. Among the suitable options, CSP is particularly attractive due to its dispatchability potential, low cost, and scalability,[5] based on the possibility of storing thermal energy. Interestingly, thermal energy storage (TES) costs are one order of magnitude lower than battery electrochemical energy storage (~$300–400/kWh).[6]

Thermochemical energy storage (TCES) is based on reversible chemical reactions in which energy is stored and released by forming and breaking chemical bonds or by adsorbing or releasing thermal energy. Usual processes have three stages: endothermic dissociation, product storage, and exothermic reaction. TCES systems generally have higher energy densities than sensible and latent TES.[7] Energy losses during storage time are negligible for those systems that allow products to be stored at ambient temperature, making it a technology with great potential for long-term storage applications.[8] Several TCES systems are being thoroughly investigated,

[1]University of Seville, Escuela Técnica Superior de Ingenieros, Camino de los Descubrimientos s/n, 41092 Seville, Spain

[2]Universidad Loyola Andalucía, Av. de Las Universidades S/n, Dos Hermanas, 41704 Seville, Spain

[3]Department of Energy Engineering, Politecnico di Torino, Corso Duca degli Abruzzi 24, 10129 Torino, Italy

[4]University of Seville, Laboratory of Engineering for Energy and Environmental Sustainability, Seville 41092, Spain

[5]Lead contact

*Correspondence: drodriguez4@us.es (D.A.R.-P.), ricardoch@us.es (R.C.)

https://doi.org/10.1016/j.xcrp.2023.101357

from laboratory prototypes to pilot scale,[9] based on hydroxides,[10] metal redox,[11] carbonates,[12–14] ammonia,[15,16] or CH_3OH[17] systems. The turning temperature at which a reversible reaction occurs is of interest. A low endothermic reaction temperature allows the use of CSP solar receivers with low concentration ratios, with consequent advantages in costs and maturity. Even renewable energy sources, such as PV and wind power, could be integrated. In contrast, high-temperature exothermic reactions ensure high-exergy heat fluxes during the discharge phase.

CH_3OH decomposition is a promising candidate for TCES for the following reasons: (1) the endothermic reaction occurs with a high conversion rate at <350°C, which involves a suitable integration with low-cost Fresnel or parabolic trough receivers when integrating the energy storage system in CSP plants; (2) the exothermic reaction (energy release) occurrs at high temperature (>500°C); (3) once CH_3OH-derived syngas is stored, several routes can be followed depending on operation strategies: syngas to CH_3OH, syngas to CH_4, or syngas to CH_4 to CH_3OH; (4) catalysts are well known at both laboratory and industrial scales[18]; (5) well-known plug-flow packed-bed reactors can be used for the reactions; (6) unlike gas-solid TCES, the system is more straightforward, avoiding the use of immature systems such as solar particle receivers, heat exchangers, or high-temperature lock hoppers; (7) a high enthalpy of reaction, which, in addition to the possibility of storing the products in liquid and pressurized gas, guarantees a high energy density of the system; (8) CH_3OH is clean and cheap, and it can be stored and delivered conveniently[19]; (9) fast kinetics to rapidly absorb solar energy and release the stored heat[20]; (10) the streams of gas and liquids can be handled with well-known commercial technologies; and (11) no side reactions occur if the reaction temperatures lock. According to IRENA,[21] current CH_3OH production will increase from 100 to 500 Mt by 2050, of which 385 Mt will be produced from renewable energy. On the contrary, the prospects for natural gas tend to increase very smoothly,[22] mainly by its widespread use in high-temperature heating processes. Therefore, the proposed conversion in this article is of economic and environmental interest for the predicted 2030–2050 scenarios, offering a pathway to keep up with gas demand in the future through its production using renewable CH_3OH.

Several recent studies have analyzed CH_3OH TCES systems at the laboratory scale or based on process simulations. A comprehensive review of reactions and methods to produce syngas from CH_3OH was carried out by Garcia.[23] A detailed kinetic model for CH_3OH synthesis was carried out on a commercial $Cu/ZnO/Al_2O_3$ catalyst bed.[24] Bai[17] evaluated the technical feasibility of a 20 kW CH_3OH-based TCES system, including a remodeled parabolic trough (filled with $Cu/ZnO/Al_2O_3$ as a catalyst) used as an endothermic reactor in which the fed gas, CH_3OH, is successfully decomposed in the receiver at 3–5 bar and also an internal combustion engine (ICE) is directly fed with the syngas produced. In this work, a larger-scale (1 MWe) system with the combustion of the produced syngas was also simulated, estimating annual energy efficiency values without solar side losses of 33.78%. The same concept was tested on a 100 kWe prototype scale by Liu[25] where the CH_3OH conversion rate exceeded 80% and a solar-to-electric efficiency of 24.73% was achieved. In these configurations, a high-temperature exhaust gas exiting the ICE could be used to preheat CH_3OH entering the reactor or for other high-temperature applications, that is, to produce cooling and heating energies through a double-effect $LiBr\text{-}H_2O$ absorption refrigerator.[26] CH_3OH would also be produced using H_2 and CO in a solar thermal cycle of cerium oxide.[27] Hong[28] proposed the combustion of CH_3OH decomposition products in an open syngas-fueled combined cycle with a net solar-to-electric efficiency of 35%. The performance of hybrid thermochemical solar PV systems operating in a full solar spectrum, taking ultraviolet-visible light photons for direct solar PV production and

the visible-infrared spectrum for thermochemical decomposition of CH_3OH, is a relevant research line with solar-to-electric efficiencies of up to 38%–45%.[20,29–33]

This article proposes a novel TCES process configuration based on different routes to obtain CH_4 and CH_3OH based on endothermic and exothermic reactions. It is based on a novel integration of reactions studied and experimentally validated in the literature. The system can operate in an open loop or as a closed-cycle TCES system. CH_4, the main component of natural gas, is used in various industrial processes ranging from heating to electricity generation and as a raw material in the chemical industry.[34] CH_3OH is widely used as a feedstock to produce other chemicals.[21] Also, it is considered fuel for ICEs[35] and biodiesel production. Comparing CH_3OH and CH_4 as fuels, CH_4 presents a higher energy density (50 MJ/kg CH_4 > 19.9 MJ/kg CH_3OH[36]) and a higher industrial maturity. On the other hand, the costs associated with transporting CH_4 are higher due to a lower energy density (0.0364 MJ/L CH_4 < 15.6 MJ/L CH_3OH[36]) than CH_3OH, which is liquid under ambient conditions, and it can have favorable characteristics for transport applications and regarding product storage The concept provides different pathways for energy use, either as the feedstock for natural gas, direct heat, and power supply or stored in chemical bonds.

This flexibility in adapting the operation of the system to different energy availability and energy needs makes the novel concept highly interesting. This article presents the concept by integrating concentrated solar energy for CH_3OH decomposition (route 1). Renewable electricity, from PV or wind power, is considered for the compression of the syngas produced to achieve an optimum high pressure in the methanation reaction. High-pressure syngas is transferred to the methanation reaction, which releases heat at high temperatures,[28] comprising route 2b. The high-temperature stream at the methanation reactor outlet can be used in an expansion process that can be used to reduce the required compression work by 75%. The CH_4 stream removes the H_2O and is a commodity used in industries. The heat released at high temperatures in the methanation reaction can be integrated with a power system. This high versatility of the direct route allows the integration and operation of the system to be adapted to different external and energy availability requirements. The conversion of CH_4 to CH_3OH closes the cycle to provide additional flexibility if required by the operation.

This article is structured as follows. First, a description of the proposed systems is given, describing the routes and details of the conversion reactions to syngas from CH_4 and CH_3OH, after which the synthesis processes of such syngas and possible commercial catalysts and reactors are discussed. An analysis of the conversion yields for both routes is carried out, and the overall energy yields are presented, considering the charging and discharging stages. Finally, the analyses associated with the reaction temperatures of each process and the reaction pressure are carried out, proposing a techno-economic optimization for decision-making on the operating parameters of the plant.

RESULTS AND DISCUSSION

System description

The system uses renewable heat from CSP for the endothermic decomposition of CH_3OH into syngas. There are several alternatives to perform decomposition, although all occur at atmospheric or slightly pressurized pressure (<10 bar) and at temperatures generally below 350°C,[37] which guarantees optimal integration with medium-temperature solar systems. The present work evaluates the TCES system in open-loop operation mode. In an open-loop mode, CH_3OH is decomposed

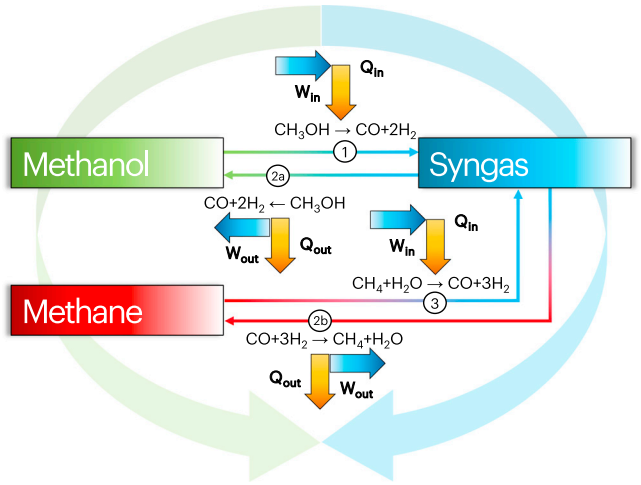

Figure 1. CH_3OH-to-CH_4-analyzed routes
A schematic outlining the routes for CH_3OH-to-CH_4 via syngas are outlined, connecting the interplays between each process.

into syngas (route 1 in Figure 1) and later converted to CH_4 (route 2b; syngas or CH_4 can be stored, providing flexibility to the system). In the open-loop operation, CH_3OH is fed constantly to the system, which produces heat, electricity, and CH_4 in different stages. This approach was proposed in the patent by Chacartegui.[38]

The closed-loop operation mode involves the regeneration of CH_3OH after energy storage occurs (syngas storage), either directly from the syngas (route 2a in Figure 1) or through the path syngas-CH_4-CH_3OH (route 3-2a), which would avoid a constant supply of CH_3OH to the system. This route adds flexibility to the system integration and operation modes if required due to system constraints.

CH_3OH to syngas

The first step is the conversion of CH_3OH to syngas, which stores energy. CH_3OH thermochemical conversion can occur via different routes: direct decomposition of CH_3OH,[17,25] steam reforming,[39] partial oxidation,[40,41] and auto thermal reforming.[42,43]

$$CH_3OH \rightarrow CO + 2H_2 \quad \Delta H_{298} = 90.7\ kJ/mol \qquad \text{(Equation 1)}$$

Direct decomposition of CH_3OH is a simple process for carrying out the conversion, as it does not require the management of O_2 and steam. It usually occurs at temperatures lower than 350°C[44] and has lower kinetics than steam reforming and oxidation.[23] According to Brown,[45] operating at 315°C and ambient pressure, complete CH_3OH conversion can be achieved using Pt/Al_2O_3-based catalyst. According to Bai,[17] CH_3OH conversion is around 95% for a solar flux using a $Cu/ZnO/Al_2O_3$ porous catalyst. The higher the pressure (up to 20 bar), the lower the temperature to reach 100% conversion to CH_3OH. A complete conversion would be obtained at atmospheric pressure and 315°C.[17] Using palladium supported on a ceria-zirconia catalyst, a complete conversion could be achieved at 200°C.[46] Plug-flow packed-bed reactors are usually proposed to perform the decomposition. Several works have proposed a packed bed-like reactor inside the parabolic trough receiver to improve solar integration to carry out endothermic reactions.[17,20,26,47]

Figure 2 illustrates the proposed conceptual scheme for the conversion of CH_3OH to syngas. Decomposition can be obtained using CSP at 300°C within a parabolic

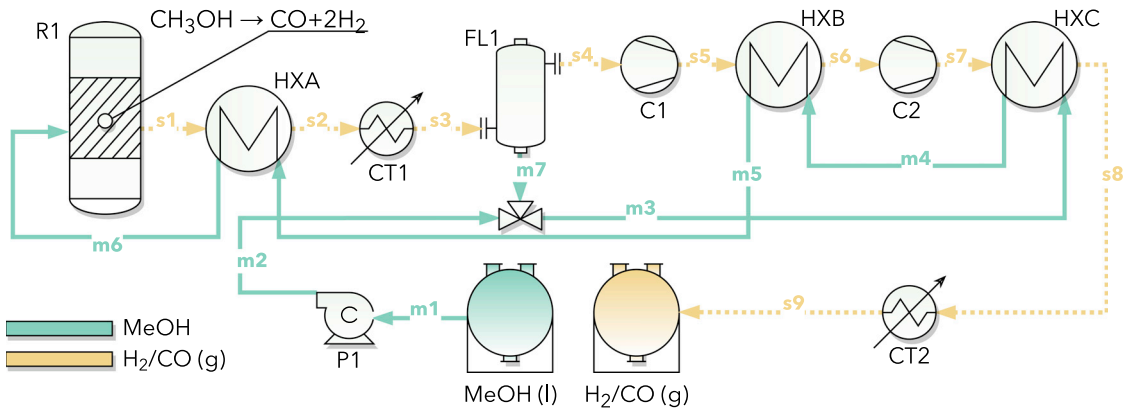

Figure 2. Conceptual scheme of the conversion of CH_3OH to syngas

Scheme outlining the route for CH_3OH to syngas as discussed in the text, where m is CH_3OH and s is syngas (CO/H_2).

trough configuration. The solar field would indirectly provide the heat required to keep the fixed bed reactor at 300°C and produce the endothermic decomposition of CH_3OH. CH_3OH enters the reactor as a compressed liquid driven by pump P1, and the reaction occurs at 10 bar to reduce the energy consumption in compressor C1. A part of the heat provided by the solar collector will be used to increase the temperature of CH_3OH and for its evaporation (~170°C). The complete conversion is assumed at the design operation. The syngas produced is further compressed to 40 bar for storage. A renewable electricity-driven intercooler compression (C1) is considered. Thus, a CSP-PV hybridization is considered for the energy storage step. If the reaction is not completed under off-design conditions, a flash separator will return the unconverted fraction of CH_3OH to the reactor in a closed loop. Before entering the endothermic reactor, CH_3OH (stream m3′) is preheated in HXA using the hot products (s1) that exit the receiver after the reaction takes place (Figure 2).

Syngas to CH_4

A relevant novelty of the concept is the approach to converting syngas to CH_4 (route 2b). Therefore, instead of using syngas directly for power conversion or CH_3OH production for energy storage (route 2a), the stored syngas can be upgraded to CH_4 for various applications. Depending on the application (CH_4 production or energy storage), it is possible to find the best trade-off between the efficiency of renewable energy storage (CSP, PV, wind) storage efficiency and the quality and quantity of syngas or CH_4 produced. This section evaluates the conversion of syngas to CH_4. Figure 3 shows the conceptual scheme for the transformation of syngas to CH_4.

$$CO + 3H_2 \rightarrow CH_4 + H_2O \quad \Delta H_{298} = -206\ kJ/mol \qquad \text{(Equation 2)}$$

Exothermic methanation converts syngas into CH_4 (Equation 2). Syngas methanation is typically carried out at temperatures between 250°C and 700°C,[48] predominantly in fixed-bed reactors.[49]

The energy discharge stage by this route (2b) begins the flow of syngas from the storage (stream s13) to send it to the methanation reactor. Energy can be recovered with a turbine in the outlet stream through the HXF and HXE preheaters (Figure 4). During the exothermic methanation reaction, the heat previously stored in chemical form is completely released at a high temperature (approximately 700°C) in an adiabatic reactor.[50] The gas exiting the reactor (stream c1) removes the heat released in methanation and drives a gas turbine to produce electricity (turbines T3–T4) that

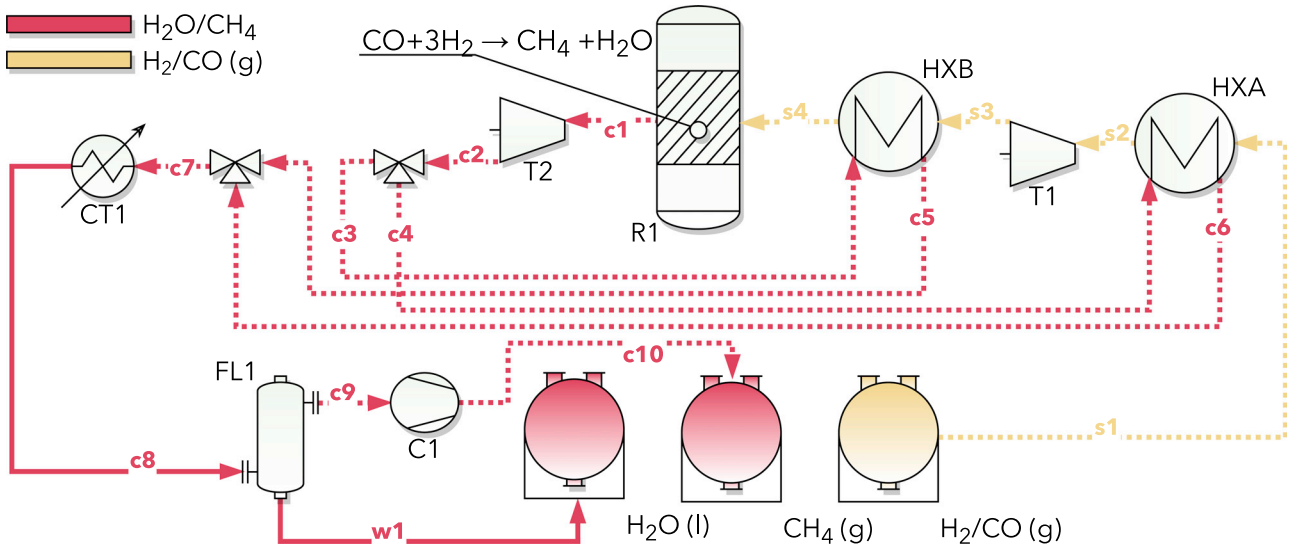

Figure 3. Conceptual scheme of syngas-to-CH_4 conversion
Outline of the process for syngas converting to CH_4, where C is CH_4, s is syngas (CO/H_2), and w is H_2O.

can be used to power compression on the CH_3OH-to-syngas route, reducing the required renewable electricity.

The CH_4 produced (c8) is stored, and it could be later used as direct feedstock for other industries, for direct combustion in high-efficiency power blocks (i.e., combined cycles), or within the thermochemical system for energy storage, evolving again to syngas (route 3) or CH_3OH (3-2a). In the direct CH_4 combustion case, the overall plant operates in an open cycle, in which the raw material is pure liquid CH_3OH under ambient conditions, and the CH_4 is ultimately burned for power production. The advantage of using CH_4 as a direct feedstock for other industries or to generate power is the use of already existing commercial technologies without requiring additional changes.

Model of the system

The proposed models are simulated in the commercial software EES[51] and the integration of the NIST-JANAF thermochemical tables.[52] The sum of all species and their respective chemical potential is shown in Equation 3, which expresses the value of the Gibbs free energy of the current in each case.[53]

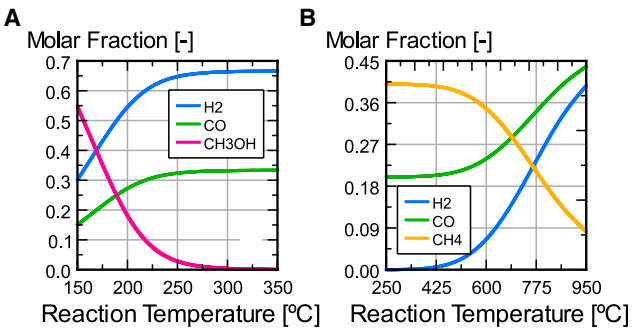

Figure 4. Mole fractions as a function of reaction temperature
Graphs depicting (A) CH_3OH decomposition (route 1) and (B) methanation (route 2b).

Table 1. Thermodynamic considerations for the proposed conversion routes, according to the charge or discharge step

Step	Variable	Value
Endothermic	CH_3OH/CH_4 inlet molar flow of the load process	100 mol/s
	CH_3OH storage temperature/pressure	64.67°C/1 bar
	syngas CO/H_2 storage pressure	40 bar
	heat exchangers approach temperatures	20 K
	isentropic efficiency of liquid CH_3OH pump	65%
	isentropic efficiency of compressors	89%
Exothermic	CH_3OH synthesis conversion	80%
	discharge pressure	1 bar
	energy storage time	10 h
	heat exchangers approach temperatures	20 K
	isentropic efficiency of turbines	92%

$$G = \sum_{k}^{n} n_k \mu_k \quad \text{(Equation 3)}$$

Analytical modeling involves the minimization of the objective function, where a conservation matrix C, a vector n of constituents, and the vector b of molar quantities are expressed at the output.

$$\min G(n)\ C^T n = b; n_k \geq 0 \forall k \quad \text{(Equation 4)}$$

In this case, the concept of Lagrangian is applied to solve the previous problem, where λ_j is the Lagrange multiplier. Where NC is the number of components, α refers to the phase and Ω to the total number of phases.

$$L = G - \sum_{j}^{NC} \lambda_j \left[\sum_{\alpha}^{\Omega} \sum_{k}^{N_\alpha} c_{kj} n_k^\alpha - b_j \right] \quad \text{(Equation 5)}$$

The equilibrium constant for the corresponding reactions is calculated from the Gibbs free energy of the chemical species in each case from Equation 6.

$$ln(k_{eq}) = \frac{-\Delta G}{RT} \quad \text{(Equation 6)}$$

Several considerations assumed for both configurations are shown in Table 1. All equipment is known in the industry and can be modeled with reasonable accuracy from zero-dimensional (lumped volume) approaches.[54,55] Models with more detailed kinetics and higher resolution may give more accurate results.[56]

The definition of the performance of the system and processes yields a global conversion efficiency, η_g, as defined in Equation 7:

$$\eta_g = \frac{m_o^{dis} X_k LHV_k + \sum_i W_i^T + \sum_i Q_{ex}}{m_i^{ch} LHV_j + \sum_i W_i^C + \sum_i Q_{endo}} = \frac{m_o^{dis} X_k \Delta h_{o,k}^{dis}}{m_i^{ch} \Delta h_{j,i}^{ch}}, \quad \text{(Equation 7)}$$

where LHV represents the lower heating value of the fuel at the inlet of the charge step, $\Delta h_o/\Delta h_i$ is the energy contained in the outlet/inlet stream, W_i^x is the compressor (C) and turbine (T) power, and Q_i is the heat of the reaction.

The conversion efficiencies η_k of any chemical species k, where j is the chemical specie at the reactor inlet (Equation 8):

$$\eta_k = \frac{m_o^k X_k \Delta h_o^k}{m_i^j \Delta h_i^j}, \quad \text{(Equation 8)}$$

Table 2. Expressions of the economic analysis of the installation

Equipment	Expression	Reference
Compressors	$IC_C = 643.15 \cdot \dot{W}_C^{0.9142}$	Carlson et al.[57]
Turbines	$IC_T = 9923.7 \cdot \dot{W}_T^{0.5886}$	Carlson et al.[57]
Pump	$IC_P = 3531.4 \cdot \dot{W}_P^{0.71} \cdot \left[1 + \left(\frac{1 - 0.8}{1 - \eta_{i,P}}\right)^3\right]$	Michalski et al.[58]
Heat exchangers	$C_{HE} = 2546.9 \cdot A_{HE}^{0.67} \cdot p_{HE}^{0.28} \cdot 10^{-6}$	Michalski et al.[58]
Endothermic reactor	$IC_{Dr} = 13140 \cdot \dot{Q}_r^{0.67}$	Michalski et al.[58]
Exothermic reactor	$IC_{Mr} = 19594 \cdot \dot{Q}_r^{0.5}$	Tesio et al.[59]
Tanks	$IC_{Tank} = 83 \cdot V$	Bayon et al.[60]

where the mass fraction X_k of the component k at the outlet of the corresponding reactor is considered. The charge η_{ch} and discharge efficiencies will be given by the amount converted in each phase between the required or exothermic energy in the processes involved (Equations 9 and 10):

$$\eta_{ch} = \frac{m_o^{ch}\left(1 - X_i^{ch}\right)\Delta h_o^{ch}}{m_i^{ch}\Delta h_i^{ch}} \quad \text{(Equation 9)}$$

$$\eta_{dis} = \frac{m_o^{dis}\left(1 - X_i^{dis}\right)\Delta h_o^{dis}}{m_i^{dis}\Delta h_i^{dis}}, \quad \text{(Equation 10)}$$

where X_i^{ch} and X_i^{dis} are the mass fractions of the components at the inlet of the charging and discharging processes, respectively.

Economic models are subject to the evolution of both component and product markets. The approximations used are based on widely used formulations for estimating early-stage technologies. The economic analysis is carried out based on the expressions shown in Table 2, which have been included in the EES programming code.

Global economic indicators are proposed, such as the levelized cost of storage (LCOS). The LCOS has been defined considering as values of the parameters a discount rate (r) of 5% and a useful life of the plant (n) of 20 years, considering the energy available Q_i^{dis} at the exit of the discharge step of both processes:

$$LCOS = \frac{CAPEX + \sum_{i=1}^{n} \frac{OPEX_i}{(1+r)^i}}{\sum_{i=1}^{n} \frac{Q_i^{dis}}{(1+r)^i}}. \quad \text{(Equation 11)}$$

$CAPEX$ is the initial investment cost of the plant, $OPEX_i$ is the annual maintenance cost, and Q_i^{dis} is the energy produced in the turbines in the exothermic phase of the proposed systems.

On-design values

The evaluation of the efficiencies described above is shown in Table 3 for the proposed operating parameters, which arise from the techno-economic optimization of the processes involved.

The efficiency results are higher in the endothermic phase than in the exothermic phase because of the complete conversion of CH_3OH and a stoichiometric defect in methanation. In any case, the proposed overall efficiency of the system as a storage system reaches 19% for its cost-benefit optimization and 22.2% for

Table 3. Results of the overall performance and thermodynamic conversion efficiency for the routes analyzed

Route	Parameter	Value
CH_3OH to syn	conversion efficiency η_{endo}	0.389
	CO production efficiency η_{CO}	0.144
	H_2 production efficiency η_{H_2}	0.266
	reaction heat (MW)	14.44
	CAPEX (M€)	24.57
Syn to CH_4	conversion efficiency η_{exo}	0.255
	reaction Heat (MW)	−15.67
	CAPEX (M€)	9.65
TCES	global efficiency η_g	0.189
	CAPEX (M€)	34.22
	OPEX (M€)	24.62
	LCOS (€/MWh)	134.8

thermodynamic optimization. Therefore, for the concluded reaction pressure and temperature parameters, the LCOS is €134.8/MWh, lower than the average for storage systems,[61] for a total investment cost of €34 million, where the phase with the highest investment is the decomposition phase. Various economic parameters will be discussed in the following section, where it has been decided to opt for a thermodynamic and cost balance to ensure correct conversion and a sufficiently rich output stream. Given the preliminary model proposed, based on the equation of state of ideal gases, the results obtained in the table above may vary by up to 8%,[62] also considering the assumptions set out in the previous section. The proposed integration is a new concept that does not present different situations, and there is no validation with a real prototype.

Sensitivity analysis

Several considerations must be made to analyze the thermochemical conversion pathways between the components studied in this article. First, the reaction temperatures should be studied because of the possible integration with CSP systems. Figure 4 shows that for the reaction pressures finally chosen (route 1: 10 bar; route 2b: 30 bar), the complete conversion of CH_3OH is obtained from 315°C, while for the endothermic phase, the low temperatures favor the synthesis into CH_4, where from above 400°C the conversion is not complete.

However, the reaction pressures will mean a variation in thermodynamic performances considering higher energy consumptions in compressors and the conditions where the syngas will have lower or higher energy at the reactor outlet. Therefore, in Figure 5A, it can be seen how higher pressures mean worse thermal efficiency at the syngas outlet in the first endothermic phase, while lower pressures increase the proposed decomposition efficiency. On the other hand, Figure 5B shows an opposite trend: the reaction yield will increase with the pressure, as the input CH_3OH has a higher enthalpy.

This analysis has also been carried out to evaluate the performance of the overall system as thermochemical storage based on the evaluation of the energy of the currents in the initial and final phases of the proposed system. Thus, Figure 5C shows that the overall performance of the system will be highly dependent on the decomposition pressure, implying that lower pressures increase the performance, as the reaction temperatures are lower. The opposite effect occurs as the pressure increases, where the reaction temperature will have to increase for maximum yield. On the

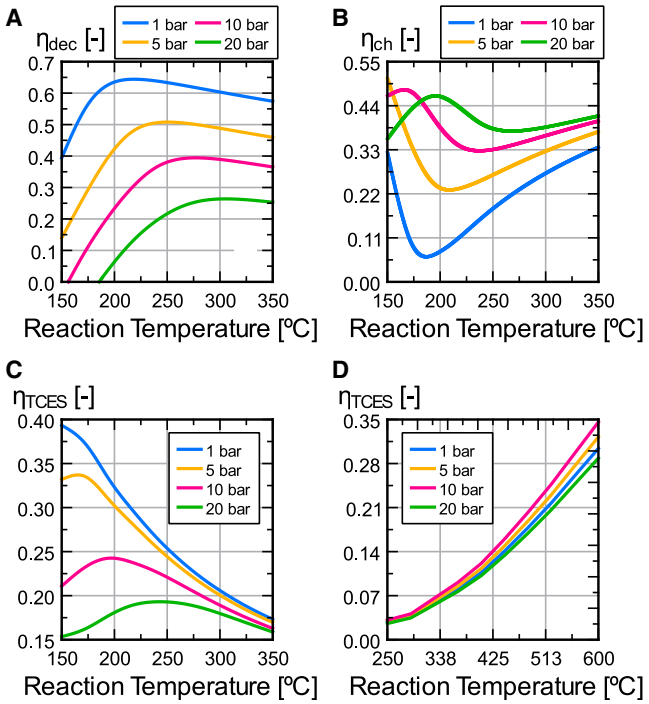

Figure 5. Thermodynamic performance efficiency as a function of reaction temperature
Graphs depicting (A) decomposition efficiency, (B) chemical conversion efficiency, (C) CH_3OH decomposition (route 1), and (D) methanation (route 2b).

other hand, in the exothermic reaction (Figure 5D), pressure does not significantly affect the overall efficiency when conversion to CH_4 is ensured, but as the temperature increases, the variation begins to become more noticeable.

Economic analysis

Despite the benefits of low pressures for reactions, the economic characterization assumes that high pressures are favored because of the savings associated with syngas compression.

The evaluation of the levelized storage cost as a function of the reaction temperature is shown in Figure 6. For route 1, the LCOS becomes minimal as the reaction temperature is lower and the pressure is higher, as discussed above. Thus, for the

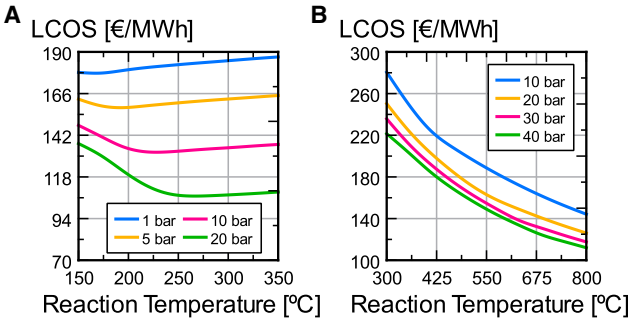

Figure 6. Levelized cost of storage (LCOS) in €/MWh as a function of reaction temperature and pressure
Graphs depicting (A) CH_3OH decomposition (route 1) and (B) methanation (route 2b).

Table 4. LCOS estimation based on TCES-CSP technology

Technology	LCOS (€/MWh)	Reference
Molten salts	280	Gautam et al.[63]
Pumped hydro	58–186	Eller[64]
Pb batteries	150–190	Jülch[65]
Li-ion	230–370	Jülch[65]
H_2	110–180	Jülch[65]
CH_4	170–260	Jülch[65]
CSP MeOH-CH_4	134.8	this work

methanation reaction, high reaction temperatures and high pressures are of interest, which will allow greater energy use in turbines and, therefore, lower consumption in compressors in the endothermic phase of the system.

Within existing energy storage technologies, the proposed system has a lower LCOS than other well-studied technologies (Table 4), such as PHS (pumped hydro storage) or Li-ion, with the levelized process costs of this article being approximately half that of CSP systems with molten salts. In this sense, the proposed model implies economic values of great interest from a storage point of view, given the high energy density of CH_3OH in the liquid state and the subsequent use of CH_4 in other processes.

A flexible CH_3OH-to-CH_4 storage system is proposed, with thermal efficiencies of up to 40% and an effluent CH_4 output with a mole fraction of over 70%, which allows direct use in existing natural gas technologies, making the system highly interesting. The ability to store liquid CH_3OH lowers transportation and storage costs due to a higher energy density than CH_4, and, in addition, decomposition temperatures (<350°C) are obtainable with CSP technologies, making the process completely CO_2 free. The reactions that take place are known in the industry, and it is shown that the high exothermic heat of methanation can be exploited by other systems. The levelized storage costs are shown to be competitive with other TCES systems at €135/MWh due to the associated savings in compressors for pumping the liquid phase CH_3OH and the simplicity of the processes involved. This article offers a novel conversion and storage system proposed as a solution for the need to obtain CH_4 from renewable and low-cost sources.

EXPERIMENTAL PROCEDURES

Resource availability

Lead contact

All requests will be fulfilled by the lead contact, Ricardo Chacartegui (ricardoch@us.es).

Materials availability

This study did not generate new materials.

Data and code availability

Any additional needs for data outside of the article will be made available by the lead contact on request.

AUTHOR CONTRIBUTIONS

Conception and design of the study, D.A.R.-P., A.C., G.M., C.O., V.V., and R.C.; acquisition of data, D.A.R.-P.; analysis and/or interpretation of data, D.A.R.-P., A.C., C.O., and R.C.; simulation, D.A.R.-P. and A.C.; writing – original draft, D.A.R.-P. and C.O.; writing – review & editing, A.C. and R.C.

DECLARATION OF INTERESTS

R.C. has patent #ES2792748A1 licensed to Universidad de Sevilla.

Received: December 5, 2022
Revised: February 1, 2023
Accepted: March 10, 2023
Published: April 3, 2023

REFERENCES

1. Lovegrove, K., James, G., Leitch, D., Milczarek, A., and Ngo, A. (2018). Comparison of Dispatchable Renewable Electricity Options: Technologies for an Orderly Transition.
2. IRENA (2019). Renewable Power Generation Costs in 2019.
3. IRENA (2020). Global Renewables Outlook: Energy Transformation 2050.
4. COP 21. UNFCCC. https://unfccc.int/process-and-meetings/conferences/past-conferences/paris-climate-change-conference-november-2015/cop-21.
5. Mehos, M., Turchi, C., Jorgensen, J., Denholm, P., Ho, C., Armijo, K., and National Laboratories, S. (2016). On the Path to SunShot: Advancing Concentrating Solar Power Technology, Performance, and Dispatchability.
6. Cole, W., Frazier, A.W., and Augustine, C. (2030). Cost Projections for Utility-Scale Battery Storage: 2021 Update.
7. Koohi-Fayegh, S., and Rosen, M.A. (2020). A review of energy storage types, applications and recent developments. J. Energy Storage *27*, 101047. https://doi.org/10.1016/J.EST.2019.101047.
8. Pinel, P., Cruickshank, C., Beausoleil-Morrison, I., and Wills, A. (2011). A Review of Available Methods for Seasonal Storage of Solar Thermal Energy in Residential Applications (Elsevier). undefined.
9. Pelay, U., Luo, L., Fan, Y., Stitou, D., and Rood, M. (2017). Thermal Energy Storage Systems for Concentrated Solar Power Plants (Elsevier). undefined. https://doi.org/10.1016/j.rser.2017.03.139ï.
10. Schmidt, M., and Linder, M. (2017). Power generation based on the Ca(OH)2/CaO thermochemical storage system – experimental investigation of discharge operation modes in lab scale and corresponding conceptual process design. Appl. Energy *203*, 594–607. https://doi.org/10.1016/J.APENERGY.2017.06.063.
11. Singh, I., and Vardhan, S. (2021). Experimental investigation of an evacuated tube collector solar air heater with helical inserts. Renew. Energy *163*, 1963–1972. https://doi.org/10.1016/J.RENENE.2020.10.114.
12. Chacartegui, R., Alovisio, A., Ortiz, C., Valverde, J.M., Verda, V., and Becerra, J.A. (2016). Thermochemical energy storage of concentrated solar power by integration of the calcium looping process and a CO2 power cycle. Appl. Energy *173*, 589–605. https://doi.org/10.1016/J.APENERGY.2016.04.053.
13. Chacartegui, R., Alovisio, A., Ortiz, C., Valverde, J.M., Verda, V., and Becerra, J.A. Thermochemical Energy Storage of Concentrated Solar Power by Integration of the Calcium Looping Process and a CO2 Power Cycle. Elsevier.
14. Ortiz, C., Valverde, J., Chacartegui, R., Perez-Maqueda, L.A., and Giménez, P. (2019). The Calcium-Looping (CaCO3/CaO) Process for Thermochemical Energy Storage in Concentrating Solar Power Plants (Elsevier).
15. Chen, C., Aryafar, H., Lovegrove, K., and Lavine, A.S. (2017). Modeling of Ammonia Synthesis to Produce Supercritical Steam for Solar Thermochemical Energy Storage (Elsevier).
16. Walmsley, T.G., Varbanov, P.S., Su, R., Klemeš, J.J., Masci, G., Ortiz, C., Chacartegui, R., Verda, V., and Valverde, J.M. (2018). The ammonia looping system for mid-temperature thermochemical energy storage*70*. https://doi.org/10.3303/CET1870128. idus.us.es.
17. Bai, Z., Liu, Q., Lei, J., and Jin, H. (2018). Investigation on the Mid-temperature Solar Thermochemical Power Generation System with Methanol Decomposition (Elsevier).
18. Shamsul, N.S., Kamarudin, S.K., Rahman, N.A., and Kofli, N.T. (2014). An overview on the production of bio-methanol as potential renewable energy. Renew. Sustain. Energy Rev. *33*, 578–588. https://doi.org/10.1016/J.RSER.2014.02.024.
19. Yan, T., Wang, R., Li, T., Wang, L., and Fred, I.T. (2015). A Review of Promising Candidate Reactions for Chemical Heat Storage (Elsevier).
20. Fang, J., Liu, Q., Guo, S., Lei, J., and Jin, H. (2019). Spanning Solar Spectrum: A Combined Photochemical and Thermochemical Process for Solar Energy Storage (Elsevier).
21. Irena And Methanol Institute (2021). Innovation Outlook (Renewable Methanol).
22. Garcia, G., Arriola, E., Chen, W.H., and de Luna, M.D. (2021). A comprehensive review of hydrogen production from methanol thermochemical conversion for sustainability. Energy *217*, 119384. https://doi.org/10.1016/J.ENERGY.2020.119384.
23. Garcia, G., Arriola, E., Chen, W., and De Luna, M.D. (2021). A Comprehensive Review of Hydrogen Production from Methanol Thermochemical Conversion for Sustainability (Elsevier).
24. Liu, T., Bai, Z., Zheng, Z., Liu, Q., Lei, J., Sui, J., and Jin, H. (2019). 100 kWe power generation pilot plant with a solar thermochemical process: design, modeling, construction, and testing. Appl. Energy *251*, 113217. https://doi.org/10.1016/J.APENERGY.2019.05.020.
25. Liu, T., Bai, Z., Zheng, Z., Liu, Q., Lei, J., Sui, J., and Jin, H. (2019). 100 kWe Power Generation Pilot Plant with a Solar Thermochemical Process: Design, Modeling, Construction, and Testing (Elsevier).
26. Bai, Z., Liu, Q., Gong, L., and Lei, J. (2019). Application of a Mid-/low-temperature Solar Thermochemical Technology in the Distributed Energy System with Cooling, Heating and Power Production (Elsevier).
27. Monnerie, N., Gan, P., Roeb, M., and Sattler, C. (2020). Methanol Production Using Hydrogen from Concentrated Solar Energy (Elsevier). https://doi.org/10.1016/j.ijhydene.2019.12.200.
28. Hong, H., Jin, H., Ji, J., Wang, Z., and Cai, R. (2005). Solar Thermal Power Cycle with Integration of Methanol Decomposition and Middle-Temperature Solar Thermal Energy (Elsevier).
29. Li, W., and Hao, Y. (2017). Efficient Solar Power Generation Combining Photovoltaics and Mid-/low-temperature Methanol Thermochemistry (Elsevier). undefined.
30. Li, W., Ling, Y., Liu, X., and Hao, Y. (2017). Performance Analysis of a Photovoltaic-Thermochemical Hybrid System Prototype (Elsevier).
31. Li, W., Hao, Y., Wang, H., Liu, H., and Sui, J. (2017). Efficient and Low-Carbon Heat and Power Cogeneration with Photovoltaics and Thermochemical Storage (Elsevier).
32. Ling, Y., Li, W., Jin, J., Yu, Y., Hao, Y., and Jin, H. (2020). A Spectral-Splitting Photovoltaic-Thermochemical System for Energy Storage and Solar Power Generation (Elsevier).
33. Qu, W., Xing, X., Cao, Y., Liu, T., Hong, H., and Jin, H. (2020). A Concentrating Solar Power System Integrated Photovoltaic and Mid-temperature Solar Thermochemical Processes (Elsevier).
34. IEA (2022). World Energy Outlook 2022.
35. Verhelst, S., Turner, J.W., Sileghem, L., and Vancoillie, J. (2019). Methanol as a fuel for internal combustion engines. Prog. Energy Combust. Sci. *70*, 43–88. https://doi.org/10.1016/J.PECS.2018.10.001.
36. CRC Handbook of Chemistry and Physics (2016). CRC Handbook of Chemistry and Physics. https://doi.org/10.1201/9781315380476.

37. Bai, Z., Liu, Q., Gong, L., and Lei, J. (2019). Application of a mid-/low-temperature solar thermochemical technology in the distributed energy system with cooling, heating and power production. Appl. Energy *253*, 113491. https://doi.org/10.1016/J.APENERGY.2019.113491.

38. Chacartegui Ramírez, R., Becerra Villanueva, J.A., Valverde Millán, J.M., Ortiz Domínguez, C., and Masci, G. (2019). ES2792748B2 - Instalacion de almacenamiento de energia termoquimicamecanica y procedimiento de almacenamiento de energia.

39. Palo, D.R., Dagle, R.A., and Holladay, J.D. (2007). Methanol steam reforming for hydrogen production. Chem. Rev. *107*, 3992–4021. https://doi.org/10.1021/CR050198B.

40. Chen, W., and Shen, C.T. (2016). Partial Oxidation of Methanol over a Pt/Al2O3 Catalyst Enhanced by Sprays (Elsevier).

41. Agrell, J., Hasselbo, K., Jansson, K., Järås, S.G., and Boutonnet, M. (2001). Production of Hydrogen by Partial Oxidation of Methanol over Cu/ZnO Catalysts Prepared by Microemulsion Technique (Elsevier).

42. Chen, W., and Lin, B.J. (2013). Hydrogen Production and Thermal Behavior of Methanol Autothermal Reforming and Steam Reforming Triggered by Microwave Heating (Elsevier).

43. Gao, J., Guo, J., Liang, D., Hou, Z., Fei, J., and Zheng, X. (2008). Production of Syngas via Autothermal Reforming of Methane in a Fluidized-Bed Reactor over the Combined CeO2–ZrO2/SiO2 Supported Ni Catalysts (Elsevier).

44. Pettersson, L., and Sjöström, K. (1991). Decomposed methanol as a fuel—a review. Combust. Sci. Technol. *80*, 265–303. https://doi.org/10.1080/00102209108951788.

45. Brown, J., and Gulari, E. (2004). Hydrogen Production from Methanol Decomposition over Pt/Al2O3 and Ceria Promoted Pt/Al2O3 Catalysts (Elsevier). undefined. https://doi.org/10.1016/j.catcom.2004.05.008.

46. Liu, Y., Hayakawa, T., Ishii, T., Kumagai, M., Yasuda, H., Suzuki, K., Hamakawa, S., and Murata, K. (2001). Methanol Decomposition to Synthesis Gas at Low Temperature over Palladium Supported on Ceria–Zirconia Solid Solutions (Elsevier).

47. Cheng, Z., Leng, Y., Men, J., and He, Y.L. (2020). Numerical Study on a Novel Parabolic Trough Solar Receiver-Reactor and a New Control Strategy for Continuous and Efficient Hydrogen Production (Elsevier).

48. Yang, L., and Ge, X. (2016). Biogas and syngas upgrading. Advances in Bioenergy *1*, 125–188. https://doi.org/10.1016/BS.AIBE.2016.09.003.

49. Hussain, I., Jalil, A.A., Hassan, N.S., and Hamid, M.Y.S. (2021). Recent advances in catalytic systems for CO2 conversion to substitute natural gas (SNG): perspective and challenges. J. Energy Chem. *62*, 377–407. https://doi.org/10.1016/J.JECHEM.2021.03.040.

50. From Solid Fuels to Substitute Natural Gas (SNG) Using TREMP™ Topsøe Recycle Energy-Efficient Methanation Process. Department of Energy.

51. Klein, K.A., and Alvarado, F.L. (2004). EES-engineering Equation Solver (F-Chart Software).

52. Chase, M. (1998). NIST-JANAF Thermochemical Tables.

53. Koukkari, P., and Pajarre, R. (2006). Calculation of constrained equilibria by Gibbs energy minimization. Calphad *30*, 18–26. https://doi.org/10.1016/J.CALPHAD.2005.11.007.

54. Formica, M., Frigo, S., and Gabbrielli, R. (2016). Development of a new steady state zero-dimensional simulation model for woody biomass gasification in a full scale plant. Energy Convers. Manag. *120*, 358–369. https://doi.org/10.1016/J.ENCONMAN.2016.05.009.

55. Lotrič, A., Sekavčnik, M., and Hočevar, S. (2014). Effectiveness of heat-integrated methanol steam reformer and polymer electrolyte membrane fuel cell stack systems for portable applications. J. Power Sources *270*, 166–182. https://doi.org/10.1016/J.JPOWSOUR.2014.07.072.

56. Couto, N., Silva, V., Monteiro, E., Brito, P.S.D., and Rouboa, A. (2015). Modeling of fluidized bed gasification: assessment of zero-dimensional and CFD approaches. J. Therm. Sci. *24*, 378–385. https://doi.org/10.1007/S11630-015-0798-7/METRICS.

57. Carlson, M., Middleton, B.M., and Ho, C.K. (2017). Techno-economic comparison of solar-driven SCO2 Brayton cycles using component cost models baselined with vendor data and estimates. asmedigitalcollection.asme.org.

58. Michalski, S., Hanak, D., and Manovic, V. (2019). Techno-economic Feasibility Assessment of Calcium Looping Combustion Using Commercial Technology Appraisal Tools (Elsevier).

59. Tesio, U., Guelpa, E., and Verda, V. (2020). Integration of Thermochemical Energy Storage in Concentrated Solar Power. Part 1: Energy and Economic Analysis/optimization (Elsevier).

60. Bayon, A., Bader, R., Jafarian, M., Fedunik-Hofman, L., Sun, Y., Hinkley, J., Miller, S., and Lipiński, W. (2018). Techno-economic Assessment of Solid–Gas Thermochemical Energy Storage Systems for Solar Thermal Power Applications (Elsevier).

61. Schmidt, O., Melchior, S., Hawkes, A., and Staffell, I. (2019). Projecting the future levelized cost of electricity storage technologies. Joule *3*, 81–100. https://doi.org/10.1016/J.JOULE.2018.12.008.

62. Øyen, S., Jakobsen, H.A., Haug-Warberg, T., and Solsvik, J. (2021). Differential Gibbs and Helmholtz reactor models for ideal and non-ideal gases: applications to the SMR and methanol processes. Chem. Eng. Sci. *234*, 116257. https://doi.org/10.1016/J.CES.2020.116257.

63. Gautam, K.R., Andresen, G.B., and Victoria, M. (2022). Review and techno-economic analysis of emerging thermo-mechanical energy storage technologies. Energies *15*, 6328. https://doi.org/10.3390/EN15176328/S1.

64. Eller, A. (2019). Comparing the Costs of Long Duration Energy Storage Technologies Commissioned by National Grid Ventures Comparing the Costs of Long Duration Energy Storage Technologies.

65. Jülch, V. (2016). Comparison of electricity storage options using levelized cost of storage (LCOS) method. Appl. Energy *183*, 1594–1606. https://doi.org/10.1016/J.APENERGY.2016.08.165.